

Published in final edited form as:

J Med Chem. 2013 June 13; 56(11): 4611–4618. doi:10.1021/jm400364h.

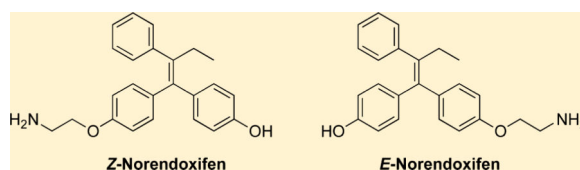
Synthesis of Mixed (*E,Z*)-, (*E*)-, and (*Z*)-Norendoxifen with Dual Aromatase Inhibitory and Estrogen Receptor Modulatory Activities

Wei Lv[†], Jinzhong Liu[‡], Deshun Lu[‡], David A. Flockhart[‡], and Mark Cushman^{*,†}

[†]Department of Medicinal Chemistry and Molecular Pharmacology, College of Pharmacy and The Purdue University Center for Cancer Research, Purdue University, West Lafayette, Indiana 47907, United States

[‡]Division of Clinical Pharmacology, Department of Medicine, Indiana University School of Medicine, Indianapolis, Indiana 46202, United States

Abstract



The first synthesis of the tamoxifen metabolite norendoxifen is reported. This included syntheses of (*E*)-norendoxifen, (*Z*)-norendoxifen, and (*E,Z*)-norendoxifen isomers. (*Z*)-Norendoxifen displayed affinity for aromatase (K_i 442 nM), estrogen receptor- α (EC_{50} 17 nM), and estrogen receptor- β (EC_{50} 27.5 nM), while the corresponding values for (*E*)-norendoxifen were aromatase (K_i 48 nM), estrogen receptor- α (EC_{50} 58.7 nM), and estrogen receptor- β (EC_{50} 78.5 nM). Docking and energy minimization studies were performed with (*E*)-norendoxifen on aromatase, and the results provide a foundation for structure-based drug design. The oral pharmacokinetic parameters for (*E,Z*)-norendoxifen were determined in mice, and (*Z*)-norendoxifen was found to result in significantly higher plasma concentrations and exposures (AUC values) than (*E*)-norendoxifen. The affinities of both isomers for aromatase and the estrogen receptors, as well as the pharmacokinetic results, support the further development of norendoxifen and its analogues for breast cancer treatment.

INTRODUCTION

Breast cancer is the most frequently diagnosed cancer in women, and it is also the second leading cause of cancer-related deaths in women in the United States. It is estimated that 226870 new cases of invasive breast cancer and 63300 new cases of in situ breast cancer occurred among women in the United States in 2012, along with 39510 breast cancer

deaths.¹ It has been established that 60% of premenopausal and 75% of postmenopausal breast cancer patients are estrogen receptor (ER) positive, with cancers that are dependent on estrogen for proliferation, making them suitable for hormonal therapy (antiestrogen treatment).² The selective estrogen receptor modulator tamoxifen (Figure 1) has been widely used for more than 30 years as the first-line hormonal therapy and adjuvant therapy after surgery for ER-positive breast cancer patients. Tamoxifen blocks ER-stimulated tumor growth in the breast, providing a 47% reduction of recurrence and 26% reduction of mortality as documented in a 5-year treatment clinical trial.³ Tamoxifen also acts as an ER agonist in bones, uterus, and other tissues, which is beneficial for preventing bone demineralization in postmenopausal women.⁴ Although the benefits are prominent, the use of tamoxifen suffers from intrinsic and acquired drug resistance, and it has only been proven to be effective for a maximum of 10 years.^{5,6} In postmenopausal women, an alternative strategy to block the effects of estrogen in promoting breast cancer is to use aromatase inhibitors (AIs) to reduce estrogen biosynthesis. Currently, three AIs (letrozole, anastrozole, and exemestane, Figure 1) have been approved for breast cancer treatment. Several clinical trials have demonstrated that the use of AIs is superior to tamoxifen in the treatment of postmenopausal women with ER-positive breast cancer. Generally, compared to tamoxifen, AIs are more effective, with increased disease-free survival, enhanced safety profile, and better tolerability.⁷⁻¹¹ However, the use of AIs is also accompanied by significant side effects, including reduction of the bone density, severe musculoskeletal pain, and increased frequency of cardiovascular and thromboembolic events.¹²⁻¹⁶ Most of these side effects of AIs have been attributed to global depletion of estrogen. There has been a need to develop new aromatase inhibitors with novel mechanisms that may cause fewer side effects.

We recently reported the human metabolism of tamoxifen to the potent aromatase inhibitor norendoxifen of undetermined stereochemistry (Figure 1).¹⁷ Norendoxifen competitively inhibits recombinant human aromatase with an IC_{50} of 90 nM. Norendoxifen also shows good selectivity toward aromatase among other CYP450 enzymes, including CYP2B6, 2C9, 2C19, 2D6, and 3A. The high potency and selectivity make norendoxifen an ideal lead compound for developing new therapeutic agents for breast cancer. Two unique features make norendoxifen attractive as a lead compound for the development of new breast cancer chemotherapeutic agents. (1) The close structural relationship of norendoxifen to tamoxifen suggests that it would be possible to make a series of compounds with dual aromatase inhibitory activity and ER modulatory activity. The aromatase inhibitory activity could efficiently block estrogen biosynthesis in the breast to inhibit the tumor growth, while the estrogen receptor modulatory activity could possibly ameliorate the side effects in bones and other tissues caused by estrogen depletion. In fact, the combination of the aromatase inhibitor anastrozole with the selective estrogen receptor modulator tamoxifen has been reported to result in fewer fractures than when anastrozole was used alone.¹⁸ (2) Because norendoxifen is a metabolite of the widely used drug tamoxifen, many patients have already been exposed to it.

This report documents the first synthesis of (*E,Z*)-norendoxifen, as well as the syntheses of (*E*)-norendoxifen (*E:Z* > 100:1) and (*Z*)-norendoxifen (*E:Z* 1:10). The aromatase inhibitory activity and ER binding affinities for mixed (*E,Z*-), as well as (*E*- and (*Z*)-norendoxifen,

were also evaluated. The possible binding mode of (*E*)-norendoxifen with aromatase was explored by molecular modeling methods. The results of these studies will facilitate future structure-based drug design efforts.

RESULTS AND DISCUSSION

Synthesis of Mixed (*E,Z*)-, (*E*)-, and (*Z*)-Norendoxifen

The syntheses of 4-hydroxytamoxifen (with a dimethylaminoethoxy side chain) and endoxifen (with a methylaminoethoxy side chain) have previously been reported.^{19–21} However, the synthesis of norendoxifen (with an aminoethoxy side chain) has not been reported in the chemical literature. This report describes the first synthesis of norendoxifen via a short and efficient synthetic pathway (Scheme 1). Starting from the 4,4'-dihydroxybenzophenone 1, the McMurry coupling reaction with propiophenone afforded the diphenol 2 in high yield (88%).¹⁹ The diphenol 2 was then monoalkylated with 2-iodoacetamide in the presence of potassium carbonate to provide the amide 3. In the last step, the reduction of the amide proceeded well with lithium aluminum hydride to afford norendoxifen 4 in high yield (82%) as a 1:1 mixture of *E*- and *Z*- isomers.

The synthesis of mixed (*E,Z*)-norendoxifen revealed that the *E*- and *Z*- isomers had strikingly different solubilities in methanol. Trituration of the solid (*E,Z*)-norendoxifen with methanol preferentially dissolved the *Z* isomer, allowing the pure (*E*)-norendoxifen (*E:Z* > 100:1) to be filtered off in nearly 40% yield (Scheme 2). The stereochemistry of (*E*)-norendoxifen was confirmed by NOE NMR spectroscopy. Irradiation of the H_a aromatic protons (Scheme 2) produced a clear NOE with the H_b benzylic methylene protons.

To prepare (*Z*)-norendoxifen, Gauthier et al.'s procedure²² was used to stereospecifically synthesize the monopivalate 6 (Scheme 3). The McMurry coupling reaction of 5²² with propiophenone provided the crude product of 6 as a mixture with *E:Z* ratio 10:1. Trituration of the crude product with methanol gave 6 as the pure *E* isomer (*E:Z* > 100) in 69% yield. In the subsequent alkylation reaction, the isomerization of 6 occurred. By minimizing the amount of reaction solvent and use of 2-iodoacetamide in excess, the crude product 7 was obtained with *E:Z* ratio 13:1. Further purification by trituration with methanol improved *E:Z* to 25:1 with 67% yield. In the last step, the reduction of the amide and removal of the pivaloyl group were accomplished in one pot. Unfortunately, partial isomerization occurred, and (*Z*)-norendoxifen (*Z*-4) was obtained with an *E:Z* ratio of 1:10. Further trituration of the product with many different solvents (including methanol, ethanol, hexanol, ethyl acetate, propanol, THF, and 2-propanol) did not improve the *E:Z* ratio.

The stabilities of (*E*)- and (*Z*)-norendoxifen in different solvents were also tested. Interestingly, if chloroform (or dichloromethane) was used as the single solvent, both (*E*)- and (*Z*)-norendoxifen underwent a fast isomerization to the mixed (*E,Z*)-norendoxifen. However, if methanol or methanol–chloroform mixture (v/v 1:1, good solubility for *E*-norendoxifen) was used as solvent, the isomerization rate was significantly decreased and the sample could be stored for at least a few weeks without substantial isomerization. This observation is similar to the isomerization of (*E,Z*)-4-hydroxytamoxifen reported by Yu et al.¹⁹ The detailed mechanism of isomerization is still not fully understood.^{23,24}

Biological Activity Evaluation

All of the compounds were tested for inhibition of aromatase activity and estrogen receptor binding affinities (including both ER- α and ER- β , Table 1). The IC₅₀ value against aromatase for the mixed (*E,Z*)-norendoxifen (4) is 102 nM, which is quite close to the value (IC₅₀ 90 nM) previously reported.¹⁷ As expected, the mixed (*E,Z*)-norendoxifen also showed good binding affinities toward both ER- α and ER- β , with EC₅₀ values in the nanomolar range (26.9 and 35.2 nM, respectively). The (*E*)-norendoxifen (*E*-4) is about 10-fold more potent than the (*Z*)-norendoxifen (*Z*-4) when tested against aromatase (IC₅₀ 77 vs 1029 nM). Because (*Z*)-norendoxifen (*E:Z* ratio 1:10) still contains a certain amount of (*E*)-norendoxifen (9%), the actual aromatase inhibitory activity for (*Z*)-norendoxifen is even weaker. For ER binding affinity, (*Z*)-norendoxifen is about 3-fold more potent than (*E*)-norendoxifen when tested against ER- α and ER- β , which is similar to the observation with 4-hydroxytamoxifen.²⁵ The aromatase inhibitory activity of diphenol 2 (IC₅₀ 25 μ M) is significantly weaker than the mixed (*E,Z*)-norendoxifen. Interestingly, the amide 3 (IC₅₀ 9.3 μ M) is also 90-fold less potent than the mixed (*E,Z*)-norendoxifen, indicating the importance of the aminoethoxy side chain for aromatase inhibition.

It was previously reported that commercial samples of (*E,Z*)-norendoxifen and (*E*)-norendoxifen had the same IC₅₀ values (90 nM) vs aromatase,¹⁷ while in the present case the IC₅₀ values of (*E,Z*)-norendoxifen (102 nM) and (*E*)-norendoxifen (77 nM) are different. During the course of the present studies, an appreciation was gained for how readily isomerization can occur and precautions were implemented to prevent it.

Molecular Modeling

A molecular docking study was performed to investigate the norendoxifen–aromatase interaction and provide a basis for further structure-based drug design. (*E*)-Norendoxifen (*E*-4) was docked into the aromatase androgen binding site (PDB 3s79) using GOLD 3.0 software, and the resulting structure was fully energy minimized using the Amber 10 molecular dynamics package. The hypothetical binding mode of (*E*)-norendoxifen in the active site of aromatase is shown in Figure 2. The phenolic hydroxyl group forms a hydrogen bond with the backbone carbonyl group of Leu372. The ether oxygen hydrogen bonds to the side chain hydroxyl group of Ser478. According to the testing results, the terminal amino group is crucial for aromatase inhibitory activity because the amide 3 is much less active than norendoxifen. Here, the amino group displayed a dual interaction with the carbonyl group (hydrogen bond) and carboxyl group (salt bridge) of Asp309. The dual interaction also explains the previous testing results that replacing the amino group with a methylamino group (endoxifen, IC₅₀ 6 μ M) or dimethylamino group (4-hydroxytamoxifen, IC₅₀ 530 μ M) significantly reduced the aromatase inhibitory activity.¹⁷ Besides the polar interactions, the unsubstituted phenyl ring and the ethyl group point toward the heme and are surrounded by hydrophobic residues Ile133 and Val370. Because this model is consistent with the aromatase inhibitory testing results for our compounds and the previously reported tamoxifen metabolites, it can provide a rational basis for further structure-based drug design.

The docking pose displayed in Figure 2 is revised relative to a previously proposed structure.¹⁷ The new pose resulted from the use of the recently released aromatase crystal

structure (PDB ID 3s79), which has slightly higher resolution than the structure used before (PDB ID 3s79 3eqm). A more significant difference is that in the present case, all crystal water molecules were removed before docking, thus making space for the aminoethoxy side chain of the ligand. According to MM-PBSA calculations, the docking pose displayed in Figure 2 has a lower calculated binding energy ($\Delta G = -46.11$ kcal/mol) than the previous structure ($\Delta G = -38.80$ kcal/mol). As stated above, this pose also has the advantage of offering an explanation for the observed decrease in aromatase inhibitory activity when the primary amino group is changed to a methylamino group or a dimethylamino group.¹⁷

Pharmacokinetics

To explore the pharmacokinetic profile and oral bioavailability for (*E*)- and (*Z*)-norendoxifen, (*E,Z*)-norendoxifen (4) was administered to NOD/SCID female mice. Plasma concentrations of (*E*)- and (*Z*)-norendoxifen were determined after a single oral dose of 100 mg/kg (Figure 3), and the pharmacokinetic parameters for both (*E*)- and (*Z*)-norendoxifen were calculated (Table 2). The results reveal that (*Z*)-norendoxifen has a more rapid absorption than (*E*)-norendoxifen (T_{\max} 1 h vs 2 h), and its peak plasma concentration is 3-fold higher than that of (*E*)-norendoxifen. The area under the curve (AUC) for (*Z*)-norendoxifen is also much higher (6-fold) than that for (*E*)-norendoxifen. However, both (*E*)- and (*Z*)-norendoxifen have similar half-lives (21.4 h vs 22.7 h), which would allow them to be tested as once daily oral agents.

The factors that could possibly contribute to the lower exposure of (*E*)-norendoxifen vs (*Z*)-norendoxifen include lower oral absorption, higher excretion rate, and a higher rate of metabolism. The possibility of lower biological exposure of (*E*)-norendoxifen resulting from its *in vivo* isomerization to (*Z*)-norendoxifen is small. The parent drug, tamoxifen, is the pure *Z* form, and patients receiving (*Z*)-tamoxifen have mainly (*Z*)-tamoxifen detected in plasma samples.²⁶ In our own work we have analyzed more than 500 tamoxifen samples from clinical trials in various settings, and we have not seen the (*E*)-tamoxifen isomer in any of these studies, even though in some cases the concentration of (*Z*)-tamoxifen was very high.

CONCLUSION

Mixed (*E,Z*)-, (*E*)-, and (*Z*)-norendoxifen have been prepared via a short and convenient synthetic approach. The mixed (*E,Z*)-norendoxifen exhibits potent aromatase inhibitory activity (IC_{50} 102 nM) while also displaying good binding affinity to both ER- α (EC_{50} 27 nM) and ER- β (EC_{50} 35 nM). (*E*)-Norendoxifen is the active component for aromatase inhibition because it is at least 10 times more active than (*Z*)-norendoxifen. In contrast, the (*Z*)-norendoxifen has slightly better binding affinity toward ER- α and ER- β than the (*E*)-norendoxifen. The possible binding mode of (*E*)-norendoxifen with aromatase was investigated by molecular modeling techniques, providing a result that can serve as the basis for further structure-based drug design. It is possible that (*E*)-norendoxifen or a closely related analogue could be an effective aromatase inhibitor with fewer side effects than aromatase inhibitors currently in use because of estrogenic effects in noncancerous cells in muscular and skeletal tissues.

EXPERIMENTAL SECTION

General

Melting points were determined using capillary tubes with a Mel-Temp apparatus and are uncorrected. The nuclear magnetic resonance (^1H and ^{13}C NMR) spectra were recorded using a Bruker ARX300 spectrometer (300 MHz) with a QNP probe or a Bruker DRX-2 spectrometer (500 MHz) with a BBO probe. High-resolution mass spectra were recorded on a double-focusing sector mass spectrometer with magnetic and electrostatic mass analyzers. The purities of biologically important compounds are 95% as determined by elemental analyses, with the observed percentages differing less than 0.40% from the calculated values. Cytochrome P450 (CYP) inhibitor screening kit for aromatase (CYP19) was purchased from BD Biosciences (San Jose, CA). Estrogen receptor α and β competitor assay kits were purchased from Invitrogen (Carlsbad, CA).

4,4'-(2-Phenylbut-1-ene-1,1-diyl)diphenol (2).¹⁹—Zinc powder (10.11 g, 154 mmol) was suspended in dry THF (100 mL), and the mixture was cooled to 0 °C. TiCl_4 (7.5 mL, 70 mmol) was added dropwise under argon. When the addition was complete, the mixture was warmed to room temperature and heated to reflux for 2 h. After cooling down, a solution of 4,4'-dihydroxybenzophenone (2.63 g, 12.3 mmol) and propiophenone (5.15 g, 38.4 mmol) in dry THF (100 mL) was added at 0 °C and the mixture was heated at reflux in the dark for 2.5 h. After being cooled to room temperature, the zinc dust was filtered off and THF was evaporated. The residue was dissolved with saturated ammonium chloride aqueous solution (150 mL) and extracted with ethyl acetate (120 mL \times 6). The organic layers were combined and dried over Na_2SO_4 , concentrated in vacuo, and further purified by silica gel column chromatography (2:1 hexanes–ethyl acetate) to provide the product 2 as yellow solid (3.4 g, 88%): mp 200–202 °C (lit.¹⁹ 200.6 °C). ^1H NMR (300 MHz, acetone- d_6) δ 7.16–7.04 (m, 7 H), 6.84–6.81 (m, 2 H), 6.70–6.67 (m, 2 H), 6.48–6.45 (m, 2 H), 2.47 (q, J = 7.5 Hz, 2 H), 0.88 (t, J = 7.5 Hz, 3 H). Anal. Calcd for $\text{C}_{22}\text{H}_{20}\text{O}_2$: C, 83.51; H, 6.37. Found: C, 83.21; H, 6.31.

(E,Z)-2-(4-(1-(4-Hydroxyphenyl)-2-phenylbut-1-enyl)phenoxy)-acetamide (3)—A suspension of 2 (3.4 g, 10.7 mmol) and K_2CO_3 (4.22 g, 30.5 mmol) in acetone (60 mL) was heated to reflux for 10 min. A solution of 2-iodoacetamide (2.4 g, 13 mmol) in acetone (20 mL) was added in small portions over 3 h, and the mixture was stirred for 1 h. After cooling down, acetone was evaporated and the residue was dissolved in saturated ammonium chloride aqueous solution (120 mL) and extracted with ethyl acetate (120 mL \times 5). The organic layers were combined, dried over Na_2SO_4 , concentrated in vacuo, and further purified by silica gel column chromatography (1:2 hexanes–ethyl acetate) to provide the product 3 as white solid (1.8 g, 45%) as a 5:4 mixture of *E* and *Z* isomers: mp 193–196 °C. ^1H NMR (500 MHz, methanol- d_4 and CDCl_3) δ 7.14–6.98 (m, 13 H), 6.91–6.89 (m, 2 H, isomer 1), 6.76–6.73 (m, 3.2 H, isomer 2), 6.63–6.61 (m, 2 H, isomer 1), 6.55–6.53 (m, 1.6 H, isomer 2), 6.40–6.38 (m, 2 H, isomer 1), 4.46 (s, 2 H, isomer 1), 4.30 (s, 1.6 H, isomer 2), 2.45–2.40 (m, 3.8 H), 0.88–0.85 (m, 5.7 H). ^{13}C NMR (125 MHz, methanol- d_4 and CDCl_3) δ 172.5, 156.0, 155.5, 155.2, 154.6, 142.4, 141.0, 140.7, 137.7, 137.5, 137.2, 134.8, 134.4, 131.8, 131.7, 130.5, 130.3, 129.4, 127.5, 125.6, 125.5, 114.6, 114.0, 113.8,

113.2, 66.6, 66.4, 28.7, 28.6, 12.9. Negative ion ESIMS m/z 372 ($M - H^+$)⁻. HRESIMS m/z calcd for C₂₄H₂₄NO₃ (MH^+) 374.1756, found 374.1749. Anal. Calcd for C₂₄H₂₃NO₃: C, 77.19; H, 6.21; N, 3.75. Found: C, 77.17; H, 6.27; N, 3.72.

(E,Z)-4-(1-(4-(2-Aminoethoxy)phenyl)-2-phenylbut-1-enyl)phenol(4)—A suspension of AlCl₃ (492 mg, 3.69 mmol) and LiAlH₄ (510 mg, 12.7 mmol) in dry THF (10 mL) was stirred under argon and cooled to 0 °C. A solution of 3 (312 mg, 0.835 mmol) in dry THF (10 mL) was added. The mixture was warmed to room temperature and stirred under argon overnight. The reaction was quenched with H₂O (3 mL), and THF was evaporated. The residue was dissolved in saturated ammonium chloride aqueous solution (20 mL) and extracted with ethyl acetate (25 mL × 4). The organic layers were combined, dried over Na₂SO₄, concentrated in vacuo, and further purified by silica gel column chromatography (1:9 methanol–dichloromethane) to provide the product **4** as a white solid (245 mg, 82%) consisting of a 5:4 mixture of *E* and *Z* isomers: mp 204–209 °C. ¹H NMR (500 MHz, CDCl₃ and methanol-d₄) δ 7.10–6.99 (m, 13 H), 6.84–6.82 (m, 2 H, *E* isomer), 6.75–6.71 (m, 3.4 H, *Z* isomer), 6.63–6.61 (m, 2 H, *E* isomer), 6.49–6.47 (m, 1.6 H, *Z* isomer), 6.40–6.39 (m, 2 H, *E* isomer), 3.99 (t, *J* = 5.1 Hz, 2 H, *E* isomer), 3.83 (t, *J* = 5.1 Hz, 1.6 H, *Z* isomer), 3.02 (t, *J* = 5.1 Hz, 2 H, *E* isomer), 2.92 (t, *J* = 5.1 Hz, 1.6 H, *Z* isomer), 2.45–2.39 (m, 3.6 H), 0.87–0.84 (m, 5.5 H). ¹³C NMR (125 MHz, CDCl₃ and methanol-d₄) δ 157.1, 156.2, 155.3, 154.4, 142.6, 142.5, 140.7, 140.5, 137.8, 136.7, 136.3, 135.0, 134.6, 131.8, 130.5, 130.4, 129.5, 127.5, 125.6, 114.6, 113.9, 113.8, 113.0, 68.5, 68.2, 40.5, 40.4, 28.7, 13.2. ESIMS m/z 360 (MH^+). HRESIMS m/z calcd for C₂₄H₂₆NO₂ (MH^+) 360.1964, found 360.1959. Anal. Calcd for C₂₄H₂₅NO₂: C, 80.19; H, 7.01; N, 3.90. Found: C, 79.98; H, 7.15; N, 3.98.

(E)-4-(1-(4-(2-Aminoethoxy)phenyl)-2-phenylbut-1-enyl)phenol(E-4)—Trituration of norendoxifen (**4**, 35 mg, *E*:*Z* = 5:4) with methanol (2 mL) gave pure (*E*)-norendoxifen (*E*-4, *E*:*Z* > 100:1) as a white solid (13.2 mg, 38%): mp 206–208 °C. ¹H NMR (300 MHz, CDCl₃ and methanol-d₄) δ 7.13–7.03 (m, 7 H), 6.88–6.85 (m, 2 H), 6.65–6.61 (m, 2 H), 6.42–6.39 (m, 2 H), 4.00 (t, *J* = 5.1 Hz, 2 H), 3.02 (t, *J* = 5.1 Hz, 2 H), 2.43 (q, *J* = 7.4 Hz, 2 H), 0.88 (t, *J* = 7.4 Hz, 3 H). ¹³C NMR (125 MHz, CDCl₃ and methanol-d₄) δ 157.2, 154.4, 142.5, 140.5, 137.8, 136.6, 134.6, 131.8, 130.4, 129.5, 127.5, 125.6, 113.9, 113.7, 69.0, 40.7, 28.7, 13.2. ESIMS m/z 360 (MH^+). HRESIMS m/z calcd for C₂₄H₂₆NO₂ (MH^+) 360.1964, found 360.1964. Anal. Calcd for C₂₄H₂₅NO₂·0.15CHCl₃: C, 76.86; H, 6.72; N, 3.71. Found: C, 76.75; H, 6.99; N, 3.49.

(E)-4-(1-(4-Hydroxyphenyl)-2-phenylbut-1-enyl)phenyl Pivalate(6).²²—Zinc powder (446 mg, 6.82 mmol) was suspended in dry THF (8 mL), and the mixture was cooled to 0 °C. TiCl₄ (0.4 mL, 3.7 mmol) was added dropwise under argon. When the addition was complete, the mixture was warmed to room temperature and heated to reflux for 2 h. After cooling down, a solution of 4-(4-hydroxybenzoyl)-phenyl pivalate (**5**, 257 mg, 0.861 mmol) and propiophenone (374 mg, 2.79 mmol) in dry THF (10 mL) was added, and the mixture was heated at reflux in the dark for 2.5 h. After being cooled to room temperature, the zinc dust was filtered off and THF was carefully evaporated. The residue was dissolved in saturated ammonium chloride aqueous solution (30 mL) and extracted with

ethyl acetate (40 mL \times 4). The organic layers were combined, dried over Na₂SO₄, concentrated in vacuo, and further purified by silica gel column chromatography (4:1 hexanes–ethyl acetate) to afford the product **6** as white solid (323 mg, 94%). The NMR spectrum showed an *E*:*Z* ratio of 10:1. Trituration with methanol (2 mL) provided the pure *E* isomer (*E*:*Z* > 100:1) as white solid (238 mg, 69%): mp 162–164 °C (lit.²² 165–167 °C). ¹H NMR (300 MHz, methanol-d₄) δ 7.25–7.22 (m, 2 H), 7.16–7.08 (m, 5 H), 7.05–7.02 (m, 2 H), 6.68–6.64 (m, 2 H), 6.42–6.39 (m, 2 H), 2.46 (q, *J* = 7.4 Hz, 2 H), 1.36 (s, 9 H), 0.91 (t, *J* = 7.4 Hz, 3 H). Anal. Calcd for C₂₇H₂₈O₃·0.8MeOH: C, 78.35; H, 7.38. Found: C, 78.26; H, 6.99.

(E)-4-(1-(4-(2-Amino-2-oxoethoxy)phenyl)-2-phenylbut-1-enyl)-phenyl Pivalate (7)

—A mixture of **6** (226 mg, 0.565 mmol), 2-iodoacetamide (434 mg, 2.35 mmol), and K₂CO₃ (440 mg, 3.18 mmol) was dissolved in acetone (8 mL). The suspension was heated to reflux and stirred for 2 h. After cooling down, acetone was carefully evaporated and the residue was dissolved in saturated ammonium chloride aqueous solution (20 mL) and extracted with ethyl acetate (20 mL \times 3). The organic layers were combined, dried over Na₂SO₄, concentrated in vacuo, and further purified by silica gel column chromatography (1:1 hexanes–ethyl acetate) to provide the product **7** as a white solid (203 mg, 78.5%). The NMR spectrum shows an *E*:*Z* ratio of 13:1. Trituration with methanol (3 mL) provided the pure *E* isomer (*E*:*Z* > 25:1) as a white solid (174 mg, 67%): mp 167–169 °C. ¹H NMR (300 MHz, CDCl₃) δ 7.26–7.20 (m, 2 H), 7.18–7.04 (m, 7 H), 6.82–6.79 (m, 2 H), 6.57–6.54 (m, 2 H), 4.35 (s, 2 H), 2.47 (q, *J* = 7.4 Hz, 2 H), 1.37 (s, 9 H), 0.92 (t, *J* = 7.4 Hz, 3 H). ¹³C NMR (75 MHz, CDCl₃) δ 177.1, 171.2, 155.0, 149.7, 142.3, 142.0, 140.8, 137.0, 136.8, 132.2, 130.4, 129.6, 127.9, 126.2, 121.2, 113.5, 66.9, 39.1, 29.0, 27.1, 13.5. ESIMS *m/z* 480 (MNa⁺). HRESIMS *m/z* calcd for C₂₉H₃₁NO₄Na (MNa⁺) 480.2151, found 480.2148. Anal. Calcd for C₂₉H₃₁NO₄: C, 76.12; H, 6.83; N, 3.06. Found: C, 75.88; H, 6.88; N, 3.06.

(Z)-4-(1-(4-(2-Aminoethoxy)phenyl)-2-phenylbut-1-enyl)phenol (Z-4)

—A suspension of AlCl₃ (135 mg, 1.01 mmol) and LiAlH₄ (195 mg, 5.14 mmol) in dry THF (5 mL) was stirred under argon and the mixture was cooled to 0 °C. A solution of **7** (95.1 mg, 0.208 mmol, *E*:*Z* > 25:1) in dry THF (5 mL) was added. The mixture was warmed to room temperature and stirred under argon for 3 h. The reaction was quenched with H₂O (0.5 mL), and THF was evaporated. The residue was dissolved in saturated ammonium chloride aqueous solution (20 mL) and extracted with ethyl acetate (20 mL \times 5). The organic layers were combined, dried over Na₂SO₄, concentrated in vacuo, and further purified by silica gel column chromatography (1:9 methanol–dichloromethane) to provide the product **Z-4** as white solid (52 mg, 70%): mp 176–179 °C. The NMR spectrum indicated an *E*:*Z* ratio of 1:10. ¹H NMR (300 MHz, methanol-d₄) δ 7.15–7.05 (m, 5.6 H), 7.03–6.98 (m, 2.2 H), 6.95–6.92 (m, 0.20 H, *E* isomer), 6.76–6.72 (m, 4 H, *Z* isomer), 6.66–6.63 (m, 0.20 H, *E* isomer), 6.58–6.54 (m, 2 H, *Z* isomer), 6.41–6.38 (m, 0.20 H, *E* isomer), 4.04 (t, *J* = 5.3 Hz, 0.20 H, *E* isomer), 3.86 (t, *J* = 5.3 Hz, 2 H, *Z* isomer), 3.03 (t, *J* = 5.3 Hz, 0.20 H, *E* isomer), 2.92 (t, *J* = 5.3 Hz, 2 H, *Z* isomer), 2.48 (q, *J* = 7.3 Hz, 2.2 H), 0.90 (t, *J* = 7.3 Hz, 3.4 H). ESIMS *m/z* 360 (MH⁺). HRESIMS *m/z* calcd for C₂₄H₂₆NO₂ (MH⁺) 360.1964, found 360.1965. Anal. Calcd for C₂₄H₂₅NO₂: C, 80.19; H, 7.01; N, 3.90. Found: C, 79.99; H, 7.08; N, 3.87.

Molecular Modeling

The structure of (*E*)-norendoxifen was constructed with Sybyl 7.1 software and energy minimized to a gradient of 0.01 kcal/mol by the Powell method using Gasteiger–Huckel charges and the Tripos force field. The crystal structure of aromatase was obtained from the Protein Data Bank (ID: 3s79), and the natural ligand (androstenedione) and all crystal water molecules were removed. The (*E*)-norendoxifen was docked into the androstenedione binding pocket in aromatase using the GOLD 3.0 program. The top five docking solutions according to the GOLD fitness score were selected, and the corresponding ligand–protein complexes were thoroughly energy minimized by the Amber 10 molecular dynamics package. The Amber parm99 force field was used for the protein during energy minimization. For the ligand, the force field parameters were taken from the General Amber Force Field (GAFF), whereas the atomic partial charges were derived from the AM1-BCC method implemented by antechamber. The ligand–protein binding energy for each energy-minimized complex was calculated using the MM-PBSA method. The complex with the lowest binding energy was selected out as the best binding pose for (*E*)-norendoxifen.

Inhibition of Recombinant Human Aromatase (CYP19) by Microsomal Incubations

The activity of recombinant aromatase (CYP19) was determined by measuring the conversion rate of fluorometric substrate 7-methoxy-4-trifluoromethylcoumarin (MFC) to its fluorescent metabolite 7-hydroxytrifluoromethylcoumarin (HFC). Experimental procedures were consistent with the published methodology.²⁷ All the incubations were performed using incubation times and protein concentrations that were within the linear range for reaction velocity. The fluorometric substrate, MFC, was dissolved in acetonitrile with the final concentration of 25 mM. All tested samples were dissolved in either methanol or methanol/dichloromethane (1:1, v/v). The sample solutions (2 μ L) were mixed well with 98 μ L of NADPH-Cofactor Mix (16.25 μ M NADP⁺, 825.14 μ M MgCl₂, 825.14 μ M glucose-6-phosphate, and 0.4 units/mL glucose-6-phosphate dehydrogenase) and were prewarmed for 10 min at 37 °C. Enzyme/substrate mix was prepared with fluorometric substrate, recombinant human aromatase (CYP19), and 0.1 M potassium phosphate buffer (pH 7.4). Reactions were initiated by adding 100 μ L of enzyme/substrate mix to bring the incubation volume to 200 μ L and incubated for 30 min. All the reactions were stopped by adding 75 μ L of 0.1 M Tris base dissolved in acetonitrile. The amount of fluorescent product was determined immediately by measuring fluorescent response using a BioTek (Winooski, VT) Synergy 2 fluorometric plate reader. Excitation–emission wavelengths for MFC metabolite were 409–530 nm. The standard curve for MFC metabolite was constructed using the appropriate fluorescent metabolite standards. Quantification of samples was performed by applying the linear regression equation of the standard curve to the fluorescence response. The limit of quantification for the metabolites of MFC was 24.7 pmol with intraand interassay coefficients of variation less than 10%.

Kinetic Analysis of Recombinant Human Aromatase (CYP19)

The rates of metabolite formation in the presence of the test inhibitors were compared with those in the control, in which the inhibitor was replaced with vehicle. The extent of enzyme inhibition was expressed as percentage of remaining enzyme activity compared to the

control. IC_{50} values were determined as the inhibitor concentrations which brought about half reduction in enzyme activity by fitting all the data to a one-site competition equation using Graphpad Prism 5.0 (GraphPad Software Inc., San Diego, CA). To characterize the inhibitory mechanism of norendoxifen against aromatase (CYP19), all inhibitory data by norendoxifen at different substrate concentrations were plotted as Lineweaver–Burk plots. The inhibitory constant K_i values were determined by nonlinear least-squares regression analysis using Graphpad Prism 5.0 (GraphPad Software Inc., San Diego, CA). Before modeling the data using nonlinear models, initial information about the inhibitory mechanism was obtained by visual inspection of Lineweaver–Burk plots. Final decision on the mechanism of inhibition was made on model-derived parameters such as R^2 (or R Square) and absolute sum of squares.

Binding Affinities for Recombinant Human Estrogen Receptor α and β (ER- α and ER- β)

The binding affinities for estrogen receptor- α and - β were determined by measuring the change of polarization value when the fluorescent estrogen ligand, ES2, was displaced by the tested compounds. Experimental procedures were consistent with the protocol provided by Invitrogen. The fluorescent estrogen ligand, ES2, was provided in methanol/water (4:1, v/v) with the concentration of 1800 nM. Recombinant human estrogen receptor- α and - β (ER- α and ER- β) were provided in buffer (50 mM bis-tris propane, 400 mM KCl, 2 mM DTT, 1 mM EDTA, and 10% glycerol), with the concentration of 734 nM and 3800 nM, respectively. All tested samples were dissolved in either methanol or methanol/dichloromethane (1:1, v/v). The sample solutions (1 μ L) were mixed well with 49 μ L of ES2 screening buffer (100 mM potassium phosphate, 100 μ g/mL BGG, and 0.02% NaN_3). The ER- α /ES2 complex was prepared with the fluorescent estrogen ligand ES2, human recombinant estrogen receptor (ER), and ES2 screening buffer with the concentration of 9 nM ES2 and 30 nM ER- α . The ER- β /ES2 complex was prepared with the fluorescent estrogen ligand ES2, human recombinant estrogen receptor- β (ER- β), and ES2 screening buffer with the concentration of 9 nM ES2 and 20 nM ER- β . Reactions were initiated by adding 50 μ L of ER/ES2 complex to bring the incubation volume to 100 μ L and incubated for 2 h avoiding light. The polarization value was determined by measuring fluorescent response using a BioTek (Winooski, VT) Synergy 2 fluorometric plate reader. Excitation–emission wavelengths for fluorescence polarization were 485–530 nm. The polarization value in the presence of the test competitors were compared with those in control in which the competitor was replaced with vehicle. The extent of competition was expressed as percentage of remaining polarization compared to the control. EC_{50} values were determined as the competitor concentrations which brought about half reduction in polarization value by fitting all the data to a one-site competition equation using Graphpad Prism 5.0 (GraphPad Software Inc., San Diego, CA).

Pharmacokinetics

The mixed (*E,Z*)-norendoxifen (100 mg/kg, *E:Z* of 45:55 determined by LC-MS-MS analysis) was given to 10-week-old NOD/SCID female mice (The Jackson Laboratory, Bar Harbor, Maine) by oral gavages according to local IUCUC approved animal protocol. Each mouse was bled for only one time point. Blood samples were collected by tail vein bleeding ($n = 3$ for each time point) at different time points up to 24 h. Plasma levels of both (*E*)-and

(Z)-norendoxifen were analyzed by LC-MS-MS method and plotted against time. The relative concentrations of *E* and *Z* isoforms are determined by their AUC in LC-MS-MS analysis. The identity of each peak was confirmed by purified *E* and *Z* isomers. Pharmacokinetic parameters were further obtained by noncompartmental modeling (Winnonlin 6.2).

Acknowledgments

This research was supported by the Purdue University Center for Cancer Research and the Indiana University Center Joint Funding Award 206330. This work was supported in part by an award from the Floss Endowment, provided to the Department of Medicinal Chemistry and Molecular Pharmacology, Purdue University. The authors acknowledge Dr. Richard F. Bergstrom for advice on pharmacokinetic analysis, and Dr. Huaping Mo for his help with NMR spectroscopy.

ABBREVIATIONS USED

AIs	aromatase inhibitors
AUC	area under the curve
ER	estrogen receptor
LAH	lithium aluminum hydride
PDB	Protein Data Bank

REFERENCES

1. Cancer Facts & Figures 2012. American Cancer Society; Atlanta: 2012.
2. Jordan VC, Brodie AM. H. Development and Evolution of Therapies Targeted to the Estrogen Receptor for the Treatment and Prevention of Breast Cancer. *Steroids*. 2007; 72:7–25. [PubMed: 17169390]
3. Davies C, Godwin J, Gray R, Clarke M, Darby S, McGale P, Wang YC, Peto R, Godwin J, Pan HC, Cutter D, Taylor C, Ingle J. Early Breast Cancer Trialists' Collaborative Group (EBCTCG). Relevance of Breast Cancer Hormone Receptors and Other Factors to the Efficacy of Adjuvant Tamoxifen: Patient-Level Meta-Analysis of Randomised Trials. *Lancet*. 2011; 378:771–784. [PubMed: 21802721]
4. Riggs BL, Hartmann LC. Drug Therapy: Selective Estrogen-Receptor Modulators—Mechanisms of Action and Application to Clinical Practice. *N. Engl. J. Med*. 2003; 348:618–629. [PubMed: 12584371]
5. Ali S, Coombes RC. Endocrine-Responsive Breast Cancer and Strategies for Combating Resistance. *Nature Rev. Cancer*. 2002; 2:101–112. [PubMed: 12635173]
6. Davies C, Pan HC, Godwin J, Gray R, Arriagada R, Raina V, Abraham M, Alencar VHM, Badran A, Bonfill X, Bradbury J, Clarke M, Collins R, Davis SR, Delmestri A, Forbes JF, Haddad P, Hou MF, Inbar M, Khaled H, Kielanowska J, Kwan WH, Mathew BS, Mitra I, Muller B, Nicolucci A, Peralta O, Pernas F, Petruzelka L, Pienkowski T, Radhika R, Rajan B, Rubach MT, Tort S, Urrutia G, Valentini M, Wang YC, Peto R. Long-Term Effects of Continuing Adjuvant Tamoxifen to 10 Years Versus Stopping at 5 Years after Diagnosis of Oestrogen Receptor-Positive Breast Cancer: ATLAS, a Randomised Trial. *Lancet*. 2013; 381:805–816. [PubMed: 23219286]
7. Bonnetierre J, Buzdar A, Nabholz JMA, Robertson JFR, Thurlimann B, von Euler M, Sahnoud T, Webster A, Steinberg M, Arimidex Writing C, Investigators Comm M. Anastrozole Is Superior to Tamoxifen as First-Line Therapy in Hormone Receptor Positive Advanced Breast Carcinoma—Results of Two Randomized Trials Designed for Combined Analysis. *Cancer*. 2001; 92:2247–2258. [PubMed: 11745278]

8. Mouridsen H, Gershanovick M, Sun Y, Perez-Carrion R, Boni C, Monnier A, Apffelstaedt J, Smith R, Sleeboom HP, Jaenicke F, Pluzanska A, Dank M, Becquart D, Bapsy PP, Salminen E, Snyder R, Chaudri-Ross H, Lang R, Wyld P, Bhatnagar A. Phase III Study of Letrozole Versus Tamoxifen as First-Line Therapy of Advanced Breast Cancer in Postmenopausal Women: Analysis of Survival and Update of Efficacy from the International Letrozole Breast Cancer Group. *J. Clin. Oncol.* 2003; 21:2101–2109. [PubMed: 12775735]
9. Nabholz JM, Bonnetterre J, Buzdar A, Robertson JFR, Thurlimann B. Arimidex Writing Comm Behalf, I. Anastrozole (Arimidex (Tm)) versus Tamoxifen as First-Line Therapy for Advanced Breast Cancer in Postmenopausal Women: Survival Analysis and Updated Safety Results. *Eur. J. Cancer.* 2003; 39:1684–1689. [PubMed: 12888362]
10. Howell A, Cuzick J, Baum M, Buzdar A, Dowsett M, Forbes JF, Hochtin-Boes G, Houghton I, Locker GY, Tobias JS, Grp AT. Results of the ATAC (Arimidex, Tamoxifen, Alone or in Combination) Trial after Completion of 5 Years' Adjuvant Treatment for Breast Cancer. *Lancet.* 2005; 365:60–62. [PubMed: 15639680]
11. Thurlimann B, Keshaviah A, Coates AS, Mouridsen H, Mauriac L, Forbes JF, Paridaens R, Castiglione-Gertsch M, Gelber RD, Rabaglio M, Smith I, Wardly A, Price KN, Goldhirsch A, Grp BI. G. C. A Comparison of Letrozole and Tamoxifen in Postmenopausal Women with Early Breast Cancer. *N. Engl. J. Med.* 2005; 353:2747–2757. [PubMed: 16382061]
12. Heshmati HM, Khosla S, Robins SP, O'Fallon WM, Melton LJ, Riggs BL. Role of Low Levels of Endogenous Estrogen in Regulation of Bone Resorption in Late Postmenopausal Women. *J. Bone Miner. Res.* 2002; 17:172–178. [PubMed: 11771665]
13. Ewer MS, Gluck S. A Woman's Heart the Impact of Adjuvant Endocrine Therapy on Cardiovascular Health. *Cancer.* 2009; 115:1813–1826. [PubMed: 19235248]
14. Bird B, Swain SM. Cardiac Toxicity in Breast Cancer Survivors: Review of Potential Cardiac Problems. *Clin. Cancer Res.* 2008; 14:14–24. [PubMed: 18172247]
15. Bundred NJ. The Effects of Aromatase Inhibitors on Lipids and Thrombosis. *Br. J. Cancer.* 2005; 93:S23–S27. [PubMed: 16100522]
16. Khan QJ, O'Dea AP, Sharma P. Musculoskeletal Adverse Events Associated with Adjuvant Aromatase Inhibitors. *J. Oncol.* 2010:8.
17. Lu WJ, Xu C, Pei ZF, Mayhoub AS, Cushman M, Flockhart DA. The Tamoxifen Metabolite Norendoxifen Is a Potent and Selective Inhibitor of Aromatase (Cyp19) and a Potential Lead Compound for Novel Therapeutic Agents. *Breast Cancer Res. Treat.* 2012; 133:99–109. [PubMed: 21814747]
18. Baum M, Buzdar AU, Cuzick J, Forbes J, Houghton J, Klijn JGM, Sahnoud T, Grp AT. Anastrozole Alone or in Combination with Tamoxifen Versus Tamoxifen Alone for Adjuvant Treatment of Postmenopausal Women with Early Breast Cancer: First Results of the ATAC Randomised Trial. *Lancet.* 2002; 359:2131–2139. [PubMed: 12090977]
19. Yu DD, Forman BM. Simple and Efficient Production of (Z)-4-Hydroxytamoxifen, a Potent Estrogen Receptor Modulator. *J. Org. Chem.* 2003; 68:9489–9491. [PubMed: 14629178]
20. Detsi A, Koufaki M, Calogeropoulou T. Synthesis of (Z)-4-Hydroxytamoxifen and (Z)-2-4-1-(P-Hydroxyphenyl)-2-Phenyl-1-Butenyl Phenoxyacetic Acid. *J. Org. Chem.* 2002; 67:4608–4611. [PubMed: 12076167]
21. Fauq AH, Maharvi GM, Sinha D. A Convenient Synthesis of (Z)-4-Hydroxy-N-desmethyltamoxifen (Endoxifen). *Bioorg. Med. Chem. Lett.* 2010; 20:3036–3038. [PubMed: 20400308]
22. Gauthier S, Mailhot J, Labrie F. New Highly Stereoselective Synthesis of (Z)-4-Hydroxytamoxifen and (Z)-4-Hydroxytoremifene via McMurry Reaction. *J. Org. Chem.* 1996; 61:3890–3893. [PubMed: 11667248]
23. Katzenellenbogen JA, Carlson KE, Katzenellenbogen BS. Facile Geometric Isomerization of Phenolic Non-Steroidal Estrogens and Antiestrogens: Limitations to the Interpretation of Experiments Characterizing the Activity of Individual Isomers. *J. Steroid Biochem. Mol. Biol.* 1985; 22:589–596.
24. Airy SC, Sinsheimer JE. Isomerization of trans-Diethylstilbestrol to Pseudo-Diethylstilbestrol. *Steroids.* 1981; 38:593–603. [PubMed: 7324087]

25. Robertson DW, Katzenellenbogen JA, Long DJ, Rorke EA, Katzenellenbogen BS, Tamoxifen Antiestrogens A. Comparison of the Activity, Pharmacokinetics, and Metabolic Activation of the Cis and Trans Isomers of Tamoxifen. *J. Steroid Biochem. Mol. Biol.* 1982; 16:1–13.
26. Murdter TE, Schroth W, Bacchus-Gerybadze L, Winter S, Heinkele G, Simon W, Fasching PA, Fehm T, Eichelbaum M, Schwab M, Brauch H. Activity Levels of Tamoxifen Metabolites at the Estrogen Receptor and the Impact of Genetic Polymorphisms of Phase I and II Enzymes on Their Concentration Levels in Plasma. *Clin. Pharmacol. Ther.* 2011; 89:708–717. [PubMed: 21451508]
27. Lu WJ, Ferlito V, Xu C, Flockhart DA, Caccamese S. Enantiomers of Naringenin as Pleiotropic, Stereoselective Inhibitors of Cytochrome P450 Isoforms. *Chirality.* 2011; 23:891–896.

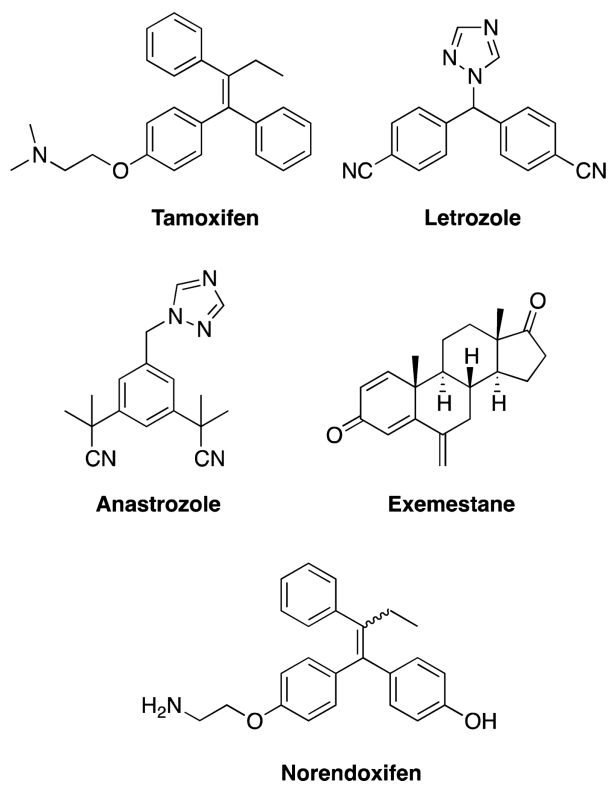
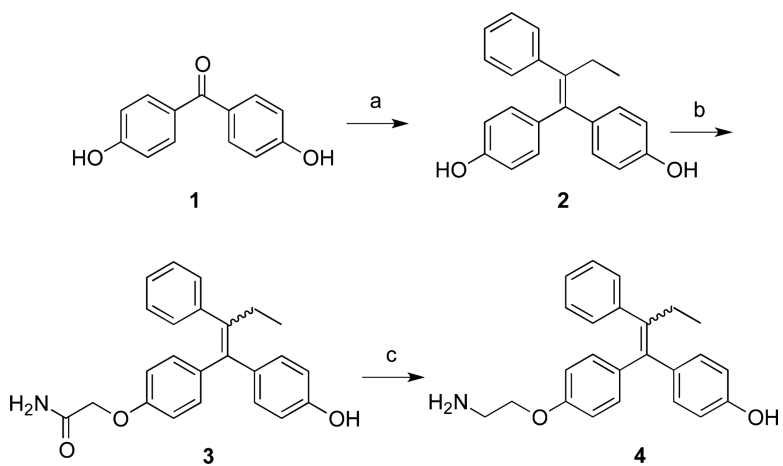
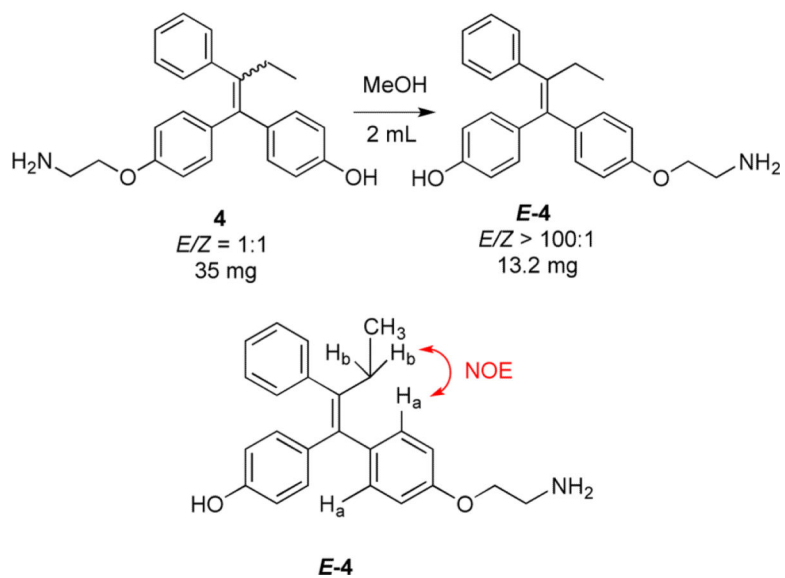


Figure 1.
The structures of the selective estrogen receptor modulator tamoxifen, the aromatase inhibitors letrozole, anastrozole, and exemestane, and the tamoxifen metabolite norendoxifen.

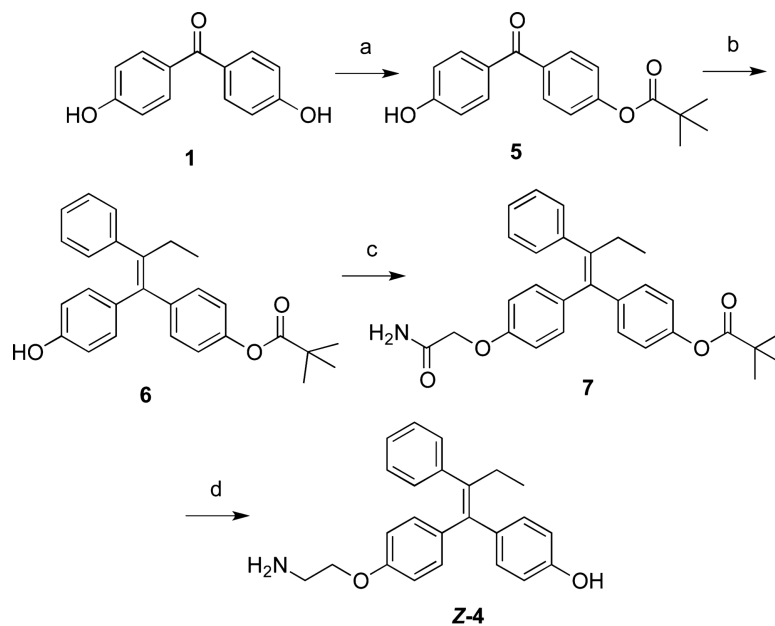


^aReagents and conditions: (a) propiophenone, Zn, TiCl₄, THF, 88%; (b) ICH₂CONH₂, acetone, K₂CO₃, 45%; (c) LAH, AlCl₃, THF, 82%.

Scheme 1.
Synthesis of Mixed (*E,Z*)-Norendoxifen 4^a



Scheme 2.
Synthesis of (*E*)-Norendoxifen (*E-4*)



^aReagents and conditions: (a) NaH, *t*-BuCOCl, THF, 36%; (b) propiophenone, Zn, TiCl₄, THF, 69%; (c) ICH₂CONH₂, acetone, K₂CO₃, 67%; (d) LAH, AlCl₃, THF, 70%.

Scheme 3.
Synthesis of (Z)-Norendoxifen (Z-4)^a

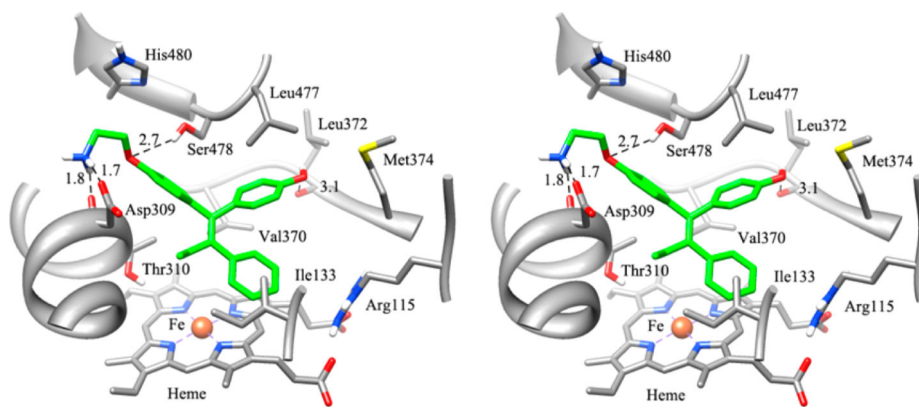


Figure 2. The hypothetical binding mode of (*E*)-norendoxifen (*E*-4, green) in the active site of human aromatase. The stereoview is programmed for wall-eyed (relaxed) viewing.

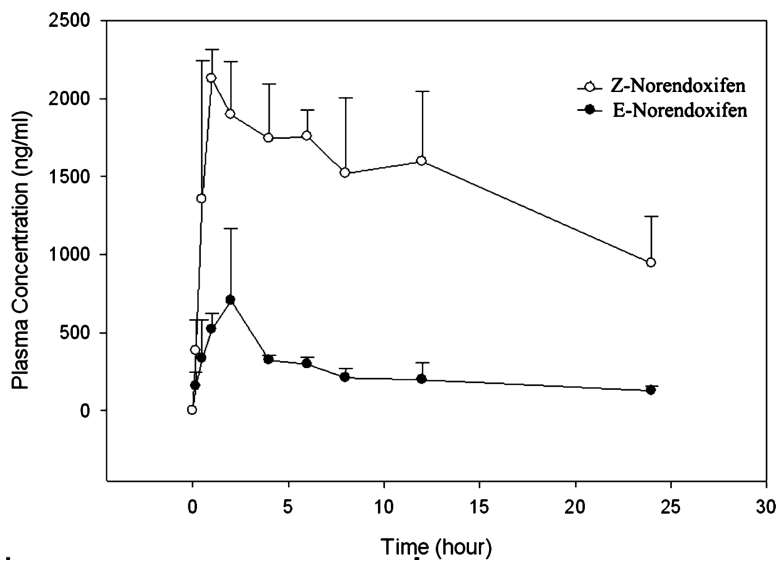


Figure 3. Time-dependent plasma concentration of (*E*)- and (*Z*)-norendoxifen following a single oral dose of the mixed (*E,Z*)-norendoxifen (100 mg/kg).

Table 1

The Aromatase Inhibitory Activity and Estrogen Receptor Binding Affinities of Norendoxifen and Structurally Related Compounds^{a,b,c,d}

compd	aromatase (IC ₅₀ , nM, or percent inhibition)	aromatase (K _i , nM)	ER- α (EC ₅₀ , nM, or percent competition)	ER- β (EC ₅₀ , nM or percent competition)
(<i>E,Z</i>)-4	102.2 ± 32.7	77 ± 9.5	26.9 ± 4.8	35.2 ± 16.8
<i>E</i> -4	76.8 ± 33.3	48 ± 0.4	58.7 ± 1.0	78.5 ± 57.3
<i>Z</i> -4	1029 ± 318	442 ± 8	17.0 ± 1.9	27.5 ± 14.3
2	24880 ± 1360	ND	80% competition	306.9 + 106.4
3	9257 ± 195	ND	57% competition	71% competition
6	8% inhibition	ND	68% competition	68% competition
7	0% inhibition	ND	56% competition	45% competition

^a ND = not determined.

^b The values are mean values of at least three experiments.

^c Percent aromatase inhibition was determined at the concentration of 50 μ M for each compound.

^d Percent estrogen receptor competition was determined at the concentration of 100 μ M for each compound.

Table 2Pharmacokinetic Parameters for (*E*)- and (*Z*)-Norendoxifen in Mice^a

compd	<i>T</i> _{max} (h)	<i>C</i> _{max} (μg/mL)	<i>C</i> _{last} (μg/mL)	<i>T</i> _{1/2} (h)	AUC _{last} (h·μg/L)	<i>V</i> _{z_F_obs} (L)	Cl _{F_obs} (L/h)
(<i>E</i>)-norendoxifen	2	0.7	0.1	21.4	5.8	2.8	0.091
(<i>Z</i>)-norendoxifen	1	2.1	0.9	22.7	35.1	0.5	0.016

^aThe data are mean concentrations in mouse plasma (*n* = 3) following a single oral dose of the mixed (*E,Z*)-norendoxifen (100 mg/kg).